STRESSES AND DISTORTIONS DURING SCAN INDUCTION CASE HARDENING OF THICK TUBE

V. Nemkov[1], R. Goldstein[1], L. Ferguson[2], Z. Li[2]
[1]Fluxtrol, Inc., 1388 Atlantic Blvd., Auburn Hills, MI 48386, USA
[2]Deformation Control Technology, Inc., Cleveland, OH, USA

ABSTRACT

Simulation of stresses during induction heat treating is a very complicated task. There are many studies of residual stresses and distortions for single shot case hardening and very few for scan hardening. This article continues a presentation of the authors at ASM conference in Cincinnati in October 2011 devoted to stress and deformation evolution for a single shot hardening of internal and external surfaces of a thick tube. Such model studies allow us to analyze the influence of basic task parameters on formation of stresses and deformation. Results of such study can help us predict and control stresses and deformations, reduce the risk of irreparable defects such as cracks, and optimize the entire process. A method of coupled simulation between electromagnetic, thermal, structural, stress and deformation phenomena during induction tube hardening is described. Software package ELTA is used to calculate the power density distribution in the load resulting from the induction heating process. The program DANTE is used to predict temperature distribution, phase transformations, stress state and deformation. Presented results demonstrate not only the residual stresses but also evolution of stresses and deformations in the process of heat treatment.

INTRODUCTION

Stress formation during induction hardening is more complicated than after furnace heating because of selective heating with high temperature gradients and a rigid core of unheated material. Scan hardening has a greater number of variables than single-shot and the process of stress and strain formation is more complicated due to accumulation of their values during the treatment process. Possibility of stress and strain simulation allows us to predict final results and optimize the induction hardening process.

Stresses and distortions during induction treatment have been under study from the very beginning of development and industrial application of this method (middle of 1930's) [1, 2]. Multiple studies have been made since that time [3-10]. For steel parts the common finding is that induction surface hardening gives compressive stresses in the martensite layer. These stresses are beneficial for component service and increase the bending strength of the part and its wear resistance [11].

However, in some cases tensile stresses may develop that reduce service properties of the component and even cause local micro or macro cracks. High stresses also lead to dimensional changes and distortions of the component. Typically these changes are undesirable, but in some cases they may be beneficial. An example of a positive role is to provide structure or size correction from induction heating, such as shrink fitting or induction straightening of large assemblies of parts [12].

Traditional descriptions of residual stress distribution after surface induction hardening of a steel bar is illustrated by Fig. 1 [13]. It shows all three components of residual stresses: radial, axial and hoop, as well as hardness distribution. In this typical case, radial stresses (σr) are much smaller than axial (σa) and hoop (σt) stresses. Hoop stresses are typically the highest and they are mainly considered in analysis. In this example, they have a maximum value of about 700 MPa (compressive) on the surface, drop to zero at the distance approximately corresponding to the case depth, change sign, reach a value of approximately 300 MPa

(tensile) at half the radius, and then drop to zero at the bar center. Tensile radial stresses may cause circular internal cracks, separating the hardened layer from the part core.

Stress evolution during heat treatment is a very complicated process and there have been no analytical methods to predict it accurately. Only experimental methods have been used, and these include dissection, x-ray, neutron, or ultrasound, all of which are labor consuming and expensive [14]. Also, methods can be applied only after process completion and important factors and effects that can occur during the process are missed.

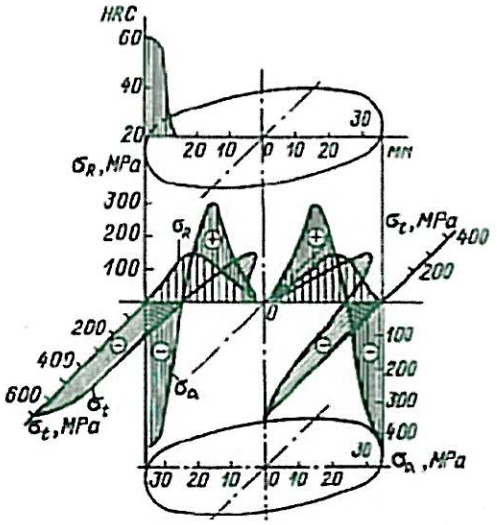

Figure 1: Typical residual stresses after hardening of steel 1045; cylinder OD is 65 mm; σt - hoop, σr – radial and σa - axial stresses; case depth is app. 6 mm.

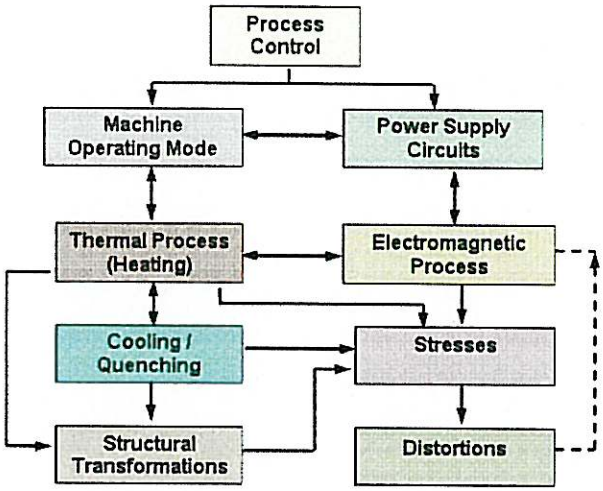

Figure 2: Chain of mutually coupled phenomena in the process of induction treatment.

Development of internal stresses and distortions resulting from induction processing has a few root causes. In the block diagram of induction heat treatment process (Fig. 2), stress and distortion blocks are at the end of a long chain of mutually coupled phenomena. The main sources of stress are mechanical, electromagnetic, thermal and microstructural. Stresses appear from the very beginning of heating due to thermal expansion of the surface layer and electrodynamic forces created by electromagnetic field on the part surface. Stresses and distortions due to electromagnetic forces are usually small compared to thermal and structural, and may be neglected except in the case of heating flat surfaces or thin long parts.

Computer simulation has been used for electromagnetic and thermal analysis for almost 40 years and has become a standard procedure for induction system design and optimization in recent years. There are multiple packages for induction system simulation. Fluxtrol, Inc. uses several programs, from the relatively simple Elta to the more complex Flux 2D/3D Finite-Element package. In combination with structural analysis, using such program as DANTE, computer simulation offers a less expensive and time consuming method for tool and process development. The accuracy of simulation and completeness of predicted information allows us to term this development procedure as "Virtual Prototyping of Induction Heat Treating"[15].

Simulation of stresses and deformation is an emerging technology, especially when dealing with induction, which started to be used for this purposes approximately 20 years ago [16-21]. Besides the variety and complexity of simulation algorithms, stress simulation requires large databases of thermal, metallurgical and mechanical properties of materials over the entire range of temperatures used during processing.

SIMULATION PROGRAMS

In the present study the induction heating software Elta was used for electromagnetic and thermal simulation and the DANTE package was used for thermal, structural, stress and distortion simulation. DANTE is finite element based software, which may be used for a complete analysis of a variety of heat treatment processes such as gear hardening after carburizing and furnace heating, quenching after furnace heating, etc. DANTE has no electromagnetic block; therefore the combination with other programs is required for simulation of the processes that contain induction heating. The DANTE software includes subroutines that mathematically describe the mechanical, thermal and metallurgical phase transformations that occur during heating and quenching of steel components so that phase fractions, hardness, dimensional change and residual stress can be predicted during the entire thermal treatment. DANTE includes a database of steel alloys that cover the common carburizing and through-hardening grades of steel. It also includes data for surface heat transfer coefficients for more commonly used quenchants and quenching methods. References [22, 23] contain more detailed information on DANTE.

Elta [24] is a program based on 1D Finite-Difference electro-thermal simulation of induction heating systems with analytical accounts for finite lengths of the part and induction coil. Elta has a database for electromagnetic and thermal properties of different materials and temperature-dependent heat transfer coefficients for a variety of quenchants. There is a special block for progressive (scan) induction heating.

SELECTION OF CASE STUDY

To minimize the number of variables and have the possibility to make a general analysis of stress and deformation evolution during heat treatment, it was decided to select a case of OD and ID induction hardening of a thick walled tube. A 4140 steel tube with an outer diameter of 28 cm, inner diameter of 16 cm and a length of 16 cm was heat treated by the scanning process using an induction coil with the length of 25 mm moving along the outer (case 1) or internal (case 2) surfaces. The heating and quenching processes were designed using Elta. The goal was to obtain a case depth of about 6-7 mm while not exceeding a maximum surface temperature of 1100°C. Optimal frequency for this hardness depth is in a range of 1-3 kHz and a frequency of 2 kHz was chosen. Calculations showed that the required heating time must be about 18 seconds which corresponds to a scanning speed of 1.39 mm/sec. Simulation showed that under these conditions the hardness depth, corresponding to a temperature of approximately 800 °C, was 6 mm for ID heating and 6.8 mm for OD heating. Process schedules are given in Table 1 and a color map of temperature distribution in the surface layer of 36 mm for outer surface is presented on Fig. 3.

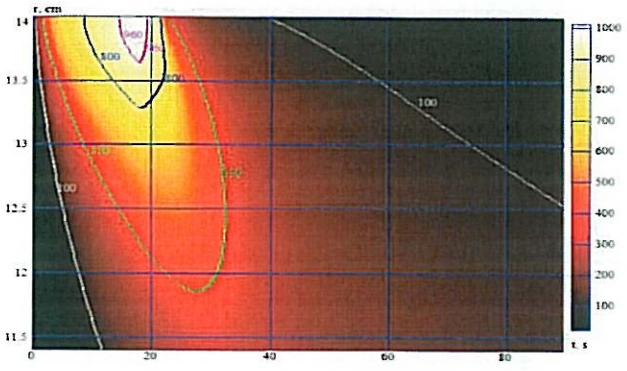

Figure 3: Color map of temperature in the surface layer of 36 mm

Table 1: Induction hardening process schedule

Step	Time sec	Frequency Hz	Power, kW	
			OD	ID
Heating	18.0	2000	100	60
Hold	3.6	-	-	-
Spray Quench*	100	-	-	-
Cooling	200	-	-	-

*12% PAG polymer solution

INDUCTION HARDENING OF TUBE OUTER SURFACE

The outer diameter surface heating example was examined first. At present time it is not possible to transfer results directly from Elta simulation into the DANTE program. The power distribution predicted by Elta was used in the DANTE model for temperature, stress, displacement and hardness calculations. A history plot of surface temperature, austenite and martensite phase fractions for a given point on the surface in the central part of the tube OD is shown in Fig. 4 from the program DANTE. Temperature fields calculated by DANTE and Elta were very similar, which confirms the accuracy of thermal blocks of both programs.

The selected point of the surface enters under the inductor face at the 52nd second after the beginning of the process and. temperature rises quickly up to approximately 1100° C during the 18-second heating time. Then tempera-ture drops due to heat soaking for 3.2 seconds before the surface point enters into the spray quenching zone. After 10 seconds of quenching the surface enters in a low intensity cooling zone, after which the final water cooling takes place. Formation of austenite occurs almost instantaneously when the surface temperature exceeds Ac3 point.

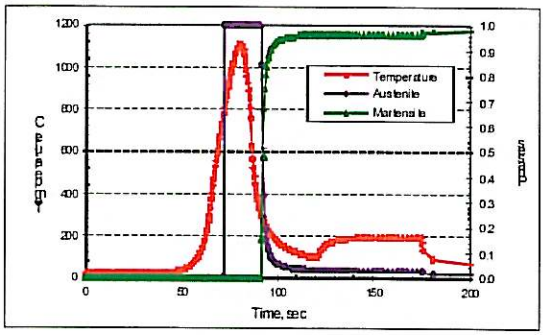

Figure 4: Temperature, austenite and martensite history from DANTE.

Conversion of austenite to martensite starts when the surface temperature drops below Ms point (about 350°C). As a result the fraction of austenite quickly drops with corresponding growth of the martensite fraction. The corresponding distributions of temperature, martensite and hoop stress are presented in Fig. 5.

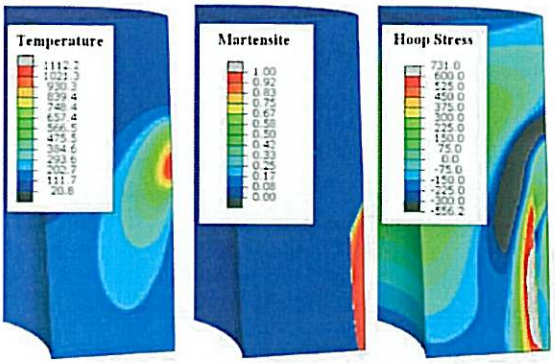

Figure 5: Snap-shot of temperature (left), martensite layer and hoop stress distribution.

The thinner layer of martensite at the start of hardening is due to the influence of axial heat transfer because of slow scanning speed. This non-uniformity may be easily corrected by power and scanning speed variation at the beginning of heating.

The development of hoop stress is rather complicated. There is a zone of strong compressive stress above and under the moving heated area. In the lower portion of the part (hardened zone), stress distribution is typical for induction surface hardening, i.e. compressive stresses on the surface followed by high tensile stresses in excess of 700 MPa. There are moderate tensile stresses on the part ID in its middle zone.

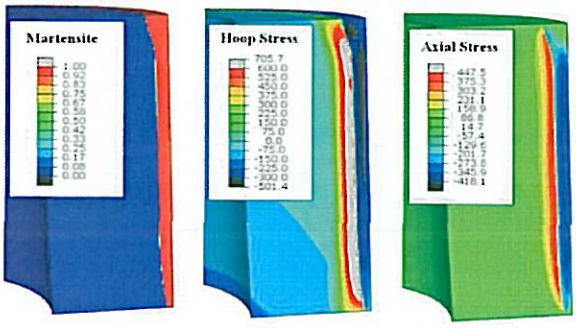

Figure 6: Distribution of martensite, hoop and axial stresses at the end of OD treatment.

A picture of stresses changes significantly during the scanning process. The distribution of martensite, hoop and axial stresses at the end of treatment of OD surface is presented in Figure 6. The thicker layer of martensite at the part top is due to

heat accumulation during the slow scanning. The hardness depth there may be corrected by control of power and scan speed. Hoop stresses near the top are higher than in the tube body, where stress distribution is typical for the surface scan hardening. Axial stresses are generally uniform in the part length, except of the very ends where they are zero due to boundary conditions.

It is important to understand stress evolution during heat treatment, especially on the part surface where tendency for cracking is highest. Figure 7 shows variation of temperature and hoop stresses on the OD surface in the middle cross-section of the parts. Rapid surface heating causes strong compressive stresses which reach -550 MPa. These stresses dissipate when the surface layer gets hot, and then become tensile (up to 200 MPa) in the process of austenite cooling before formation of martensite, which results in fast reversal of stress to compression. Penetration of a phase transformation front into the depth and thermal expansion of the rigid internal layers below the austenite layer due to further heat soaking cause the surface stress to again become tensile (the second peak in a positive range). Further variations of surface stresses are due to the overall temperature distribution in the part wall. Residual stresses on the OD surface are compressive (close to -280 MPa), which is a positive factor for the part operation in service.

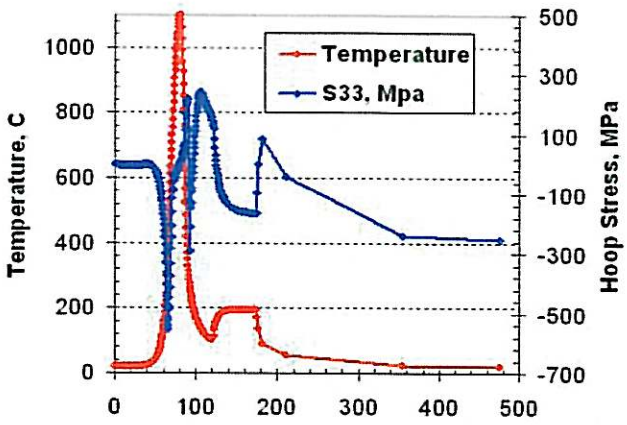

Figure 7: Evolution of temperature and hoop stresses on the part OD surface in the middle cross-section.

INDUCTION SCAN HARDENING OF INTERNAL SURFACE

The temperature distribution map at the middle of the ID scanning cycle is displayed in Fig. 8, along with the corresponding stress and martensite distributions. A large layer of compressive stress appears above and outside of the formed austenite. This compressive zone moves upward ahead of the hot zone as scanning takes place. Outside of the newly formed martensite layer is a zone of high tensile hoop stress.

The temperature, martensite and hoop stress distributions are shown in Fig. 9 at a scan time just prior to the hot zone reaching the top of the tube. The large internal compressive stress zone has reached the top ID corner. The hoop stress at the bottom ID corner has become compressive, but the hoop stress in the martensite at mid-height is tensile, with a high tensile stress being present just below the hardened case. The final stress distributions after ID quenching and cooling are displayed in Fig. 10. A layer of tensile hoop stress is present over the mid-section of the tube ID to roughly the case depth. The hoop stress at the bottom and top ID sections is compressive. The axial stress on the ID is compressive, except at the tube ends

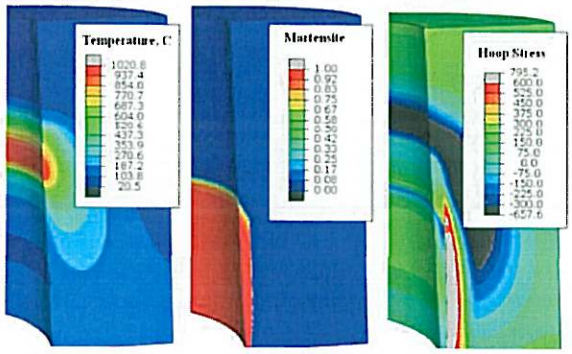

Figure 8: Distribution of temperature, martensite and hoop stresses at the middle of treatment.

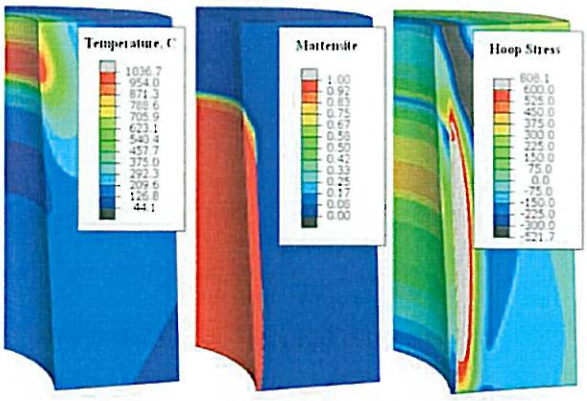

Figure 9: Distribution of temperature, martensite and axial stresses at the end of heating stage. (Dimensional change is magnified 10X)

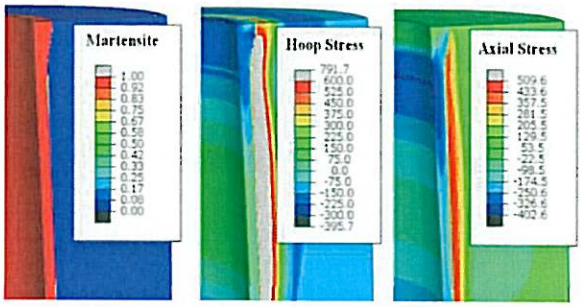

Figure 10: Distribution of martensite, hoop and axial stresses at the end of treatment. (Dimensional change is magnified 10X)

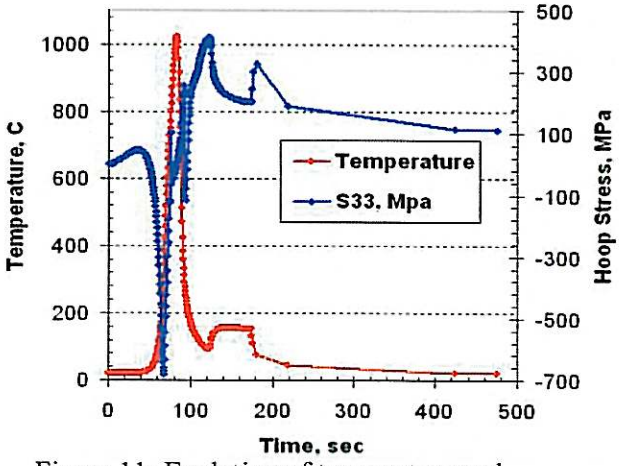

Figure 11: Evolution of temperature and hoop stresses on the part surface in the middle cross-section.

where it is zero. Both hoop and axial stresses are distributed along the tube non-uniformly. Similar to the OD scanning case, Figure 10 shows that the martensite thickness is increased at the top corner of the ID.

The compressive axial stress layer and the tensile hoop stress at mid-height on the bore of the tube is immediately backed by a layer of significant tensile stresses at depths from 7 to 15 mm. The remainder of the body maintains a slight state of hoop compression and mild axial tension.

Figure 11 shows temperature and hoop stress histories at mid-height of the bore of the tube throughout the ID scanning process. After about 50 seconds this location begins to heat and the region transitions into deep compression (-700 MPa) as thermal expansion is restricted. As austenite forms, the compression is relieved due to the crystal structure change. The austenite is stretched in tension by neighboring and underlying material expansion. Martensite formation quickly imposes hoop compression during spray cooling, but neighbor and subsurface influences reinstitute tensile stress. This bore section remains in hoop tension of about 100 MPa after process completion. This is considerably different than OD scan hardening which produced hoop surface compression.

Dimensional Changes

Figure 12 shows cross sectional comparisons of the predicted radial displacements for both OD and ID hardening using the single shot method and the scanning method. Parts A and B are for OD hardening, and parts C and D are for ID hardening. Parts A and C are for scan hardening, and B and D are for single shot hardening. The dimensional changes in these figures have been magnified twenty times so it is easier to identify the shape distortion. First looking at OD hardening, Figures 12 A & B show that the general rule is that the tube shrinks radially for both single shot and scan hardening. This makes sense in that the OD hoop stress for both

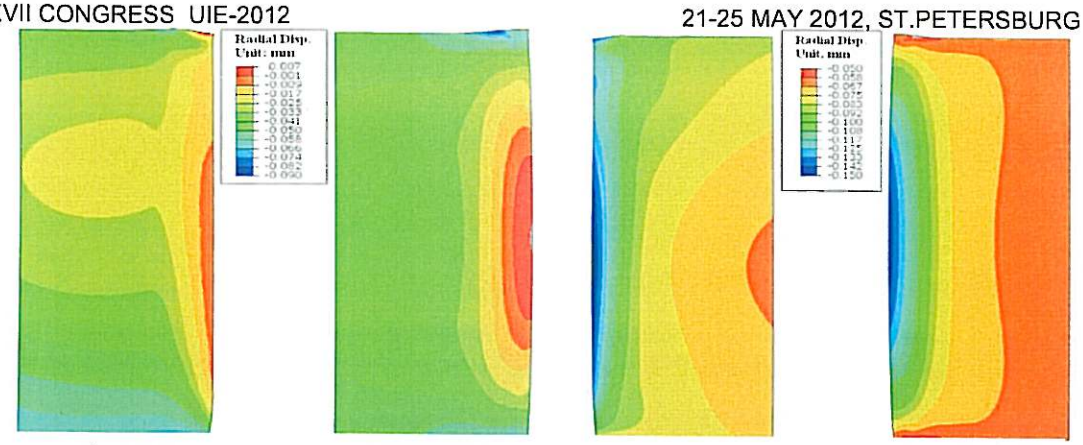

Figure 12: Radial displacement distribution at the end of cooling for OD and ID treatment. **A** and **C** – scan hardening; **B** and **D** – single-shot hardening
(Dimensional changes are magnified 20X)

cases is compressive. Single shot hardening of the OD surface, Figure 12 B, produces dimensional change that is symmetric from bottom to top and non-symmetric for scanning (Fig. 12A). Comparison of the contour patterns and the OD corner feature bears this out. The OD surface for single shot bulges more that the scan hardened OD surface, and actually is predicted to grow about 7 microns while the tube body shrinks.

For tube ID hardening, both the bore and the OD are predicted to shrink in comparison to the starting dimensions, see Figures 12 C and D. For single shot hardening, part D, the radial shrinkage of the bore is predicted to be -0.146 mm and for the outer wall it is -0.058 mm. The most significant shrinkage is predicted at mid-height of the tube ID, and this is approximately two times the radial shrinkage at the tube ends. This is also true for ID scan hardening. As for OD hardening, scan ID hardening produces non-symmetric dimensional change in the tube length.

CONCLUSIONS

Internal stresses due to temperature variation and structural transformation during induction processing may be positive (shrink-fitting, bending strength improvement) or detrimental/negative (deformations, cracks, service properties reduction). In order to achieve the desired final properties of a material, the phenomena that occurs during the cycle needs to be understood and predictable. Residual stresses and part deformation after induction surface hardening depend upon many factors: part geometry, alloy chemistry and initial microstructure of the material, case depth, heating and quenching parameters. It is very difficult to study the interaction of all these factors by empirical methods alone. Because of the many stress reversals that accompany hardening, intuition is easily fooled. Computer simulation is a powerful tool for analysis of stresses and deformation evolution during the entire processing cycle.

This study of a thick-wall tube induction treatment using the Elta and DANTE programs showed that the final stress distribution is different for ID and OD surface hardening. Hoop stress distribution along the part length is not uniform with hoop stress concentration near the tube ends for ID hardening and in the central zone for OD hardening. Dimensional distortion of the part may be significant during the treatment process even if the final deformation is small. Stress evolution shows a reversal behavior with a possibility of high tensile stresses during the martensite formation, which can lead to quenching cracks. This effect is stronger for ID hardening than for OD hardening.

REFERENCES

[1] V. Vologdin, Surface Hardening by High Frequency Currents, Metallurg, no.12, 1937 (in Russian)

[2] Kontorovich and L. Livshits, Internal residual stresses induced in steel by high-frequency surface hardening, Metallurg, No. 8, 30, 1940 (in Russian)
[3] J. Grum, Overview of residual stresses after induction surface hardening. International Journal of Materials and Product Technology, Volume 29, no.1-4, 2007
[4] M. Lozinski, Industrial Applications of Induction Heating, Pergamon Press, Oxford, 1969
[5] G. Golovin, Residual Stresses and Deformation during High-Frequency Surface Hardening, Mashghiz, Moscow, 1962 (in Russian)
[6] S. Jahanian. Thermoelastoplastic and Residual Stress Analysis during Induction Hardening of Steel, Journal of Materials Eng. and Performance, V. 4, Issue 6, 1995
[7] W. Dowling, et al., "Development of a Carburizing and Quenching Simulation Tool: Program Overview," 2nd Int. Conference on Quenching and Control of Distortion, eds, G. Totten, et al., ASM Int., 1996
[8] C. Anderson, et al., "Development of a Carburizing and Quenching Simulation Tool: Numerical Simulations of Rings and Gears," 2nd Int. Conference on Quenching and Control of Distortion, eds, G. Totten, et al., ASM Int., 1996.
[9] B. Liscic, Hardenability, in Steel Heat Treatment Handbook, edited by G. Totten and M. Howes, Marcel Dekker, NY, 1997
[10] J. Grum, Induction Hardening, in Handbook of Residual Stress and Deformation of Steel, edited by G. Totten, M. Howes, T. Inoue, ASMI, Materials Park, OH, pp 220-247, 2002
[11] Kudryavtsev, Internal Stresses as Resource of Strength in Machinary, M., Mashghiz, 1951 (in Russian)
[12] N. McPherson, Induction heat straightening – A distortion rework reduction tool for thin plates, Welding and Cutting, 7, no.23, 2008
[13] G. Golovin, Residual Stresses, Strength and Deformation during Surface Hardening by High-Frequency Currents, Mashinostroyeniye, Leningrad, 1973 (in Russian)
[14] Handbook of Measurement of Residual Stresses, Society for Experimental Mechanics, Jian Lu (Ed.): Fairmont Press, 1996
[15] R. Goldstein, V. Nemkov, J. Jackowski, Virtual Prototyping of Induction Heat Treating, Proc. of the 25th ASM Heat Treating Society Conference, Sept. 14–17, 2009
[16] D. Bammann, et al., "Development of a Carburizing and Quenching Simulation Tool: A Material Model for Carburizing Steels Undergoing Phase Transformations," 2nd Int. Conference on Quenching and Control of Distortion, ASM Int., 1996
[17] W. Dowling, et al., "Development of a Carburizing and Quenching Simulation Tool: Program Overview," 2nd International Conference on Quenching and Control of Distortion, eds, G. Totten, et al., ASM Int., 1996.
[18] H. Kristoffersen, P. Vomacka, Influence of process parameters for induction hardening on residual stresses, Materials & Design, Volume 22, Issue 8, December 2001
[19] P. Pacheco, M. Savi, A. Camara, Analysis of Residual Stresses Generated by Progressive Induction Hardening of Steel Cylinders, J. of Stain Analysis, v. 36, n. 5, 2001
[20] L. Hellenthal, C. Groth, Simulation of Residual Stresses in an Induction Hardened Roll, 23rd CADFEM Users' Meeting 2005, Int. Congress on FEM Technology, 2005
[21] C. Gur, J. Pan, Handbook of Thermal Process Modeling of Steel, CRC Press, 2009
[22] B.L Ferguson, A. Freborg, G. Petrus, M. Callabresi. Predicting the Heat-Treat Response of a Carburized Helical Gear, Gear Technology, December 2002
[23] Z. Li, A. Freborg, B. Ferguson, Application of modeling to heat treat processes. Heat Treating Processes, May/June 2008
[24] Elta (www.nsgsoft.com)